Biomedical Signal Analysis: Contemporary Methods and Applications

Fabian J. Theis and Anke Meyer-Bäse

The MIT Press
Cambridge, Massachusetts
London, England

This book was set in LaTeX by Fabian J. Theis and Anke Meyer-Bäse.

Printed and bound in the United States of America.

Library of Congress Cataloging-in-Publication Data

Theis, Fabian J.
Biomedical signal analysis: contemporary methods and applications / Fabian J. Theis and Anke Meyer-Bäse.
p. cm.
Includes bibliographical references and index.
ISBN 978-0-262-01328-4 (hardcover : alk. paper) 1. Magnetic resonance imaging. 2. Image processing. 3. Diagnostic imaging. I. Meyer-Bäse, Anke. II. Title.
RC78.7.N83T445 2009
616.07'54-dc22

10 9 8 7 6 5 4 3 2 1

1 Foundations of Medical Imaging and Signal Recording

Computer processing and analysis of medical images, as well as experimental data analysis of physiological signals, have evolved since the late 1980s from a variety of directions, ranging from signal and imaging acquisition equipment to areas such as digital signal and image processing, computer vision, and pattern recognition.

The most important physiological signals, such as electrocardiograms (ECG), electromyograms (EMG), electroencephalograms (EEG), and magnetoencephalograms (MEG), represent analog signals that are digitized for the purposes of storage and data analysis.

The nature of medical images is very broad; it is as simple as an chest X-ray or as sophisticated as noninvasive brain imaging, such as functional magnetic resonance imaging (fMRI).

While medical imaging is concerned with the interaction of all forms of radiation with tissue and the clinical extraction of relevant information, its analysis encompasses the measurement of anatomical and physiological parameters from images, image processing, and motion and change detection from image sequences.

This chapter gives an overview of biological signal and image analysis, and describes the basic model for computer-aided systems as a common basis enabling the study of several problems of medical-imaging-based diagnostics.

1.1 Biosignal Recording

Biosignals represent space-time records with one or multiple independent or dependent variables that capture some aspect of a biological event. They can be either deterministic or random in nature. Deterministic signals very often can be compact, described by syntactic techniques, while random signals are mainly described by statistical techniques.

In this section, we will present the most common biosignals and the events from which they were generated. Table 1.1 describes these signals.

Biosignals are usually divided into the following groups:

• Bioelectrical (electrophysiological) signals: Electrical and chemical transmissions form the electrophysiological communication between neu-

Table 1.1
Most common biosignals [56].

Event	Signal
Heart electrical conduction at limb surfaces	Electrocardiogram (ECG)
Surface CNS electrical activity	Electroencephalogram (EEG)
Magnetic fields of neural activity	Magnetoencephalogram (MEG)
Muscle electrical activity	Electromyogram (EMG)

ral and muscle cells. Signal transmission between cells takes place as each cell becomes depolarized relative to its resting membrane potential. These changes are recorded by electrodes in contact with the physiological tissue that conducts electricity. While surface electrodes capture bioelectric signals of groups of correlated nerve or muscle cell potentials, intracellular electrodes show the difference in electric potential across an individual cell membrane.

• Biomechanical signals: They are produced by tissue motion or force with highly correlated time-series from sample to sample, enabling an accurate modeling of the signal over long time periods.

• Biomagnetic signals: Body organs produce weak magnetic fields as they undergo electrical changes, and these biosignals can be used to produce three-dimensional images.

• Biochemical signals: They provide functional physiological information and show the levels and changes of various biochemicals. Chemicals such as glucose and metabolites can be also measured.

Electroencephalogram (EEG)

The basis of this method lies in the recording over time of the electric field generated by neural activity through electrodes attached to the scalp. The electrode at each position records the difference in potential between this electrode and a reference one. EEG is employed for spontaneous brain activity, as well as after averaging several presentations of the stimulus. These responses are processed either in the time or in the frequency domain.

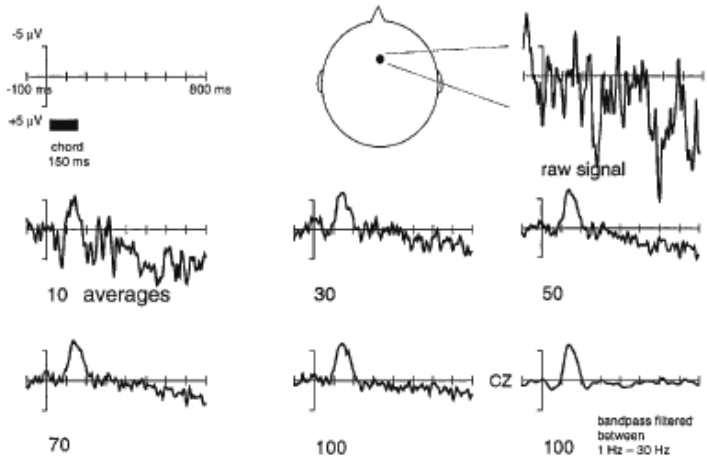

Figure 1.1
EEG signal processing. The EEG signal is displayed in the upper right corner, and the filtered signals averaged is shown below [243].

Magnetoencephalogram (MEG)

The magnetoencephalogram is a technique that records based on ultrasensitive superconducting sensors (SQUIDS), which are placed on a helmet-shaped device. The magnetic fields generated by the neural activity thus allow clinicians to monitor brain activity at different locations and represent different brain functions. As with EEG, the magnetic fields result from coherent activity of dendrites of pyramidal cells. The processing methods are the same as in EEG in regard to both spontaneous and averaged activity. Both EEG and MEG have their own advantages. In MEG, the measured magnetic fields are not affected by the conductivity boundaries, as is the case with EEG. On the other hand, EEG, compared to MEG, enables the localization of all possible orientations of neural sources.

Electrocardiogram (ECG)

The electrocardiogram (ECG) is the recording of the heart's electric activity of repolarization and depolarization of the atrial and ventricular chambers of the heart. Depolarization is the sudden influx of cations

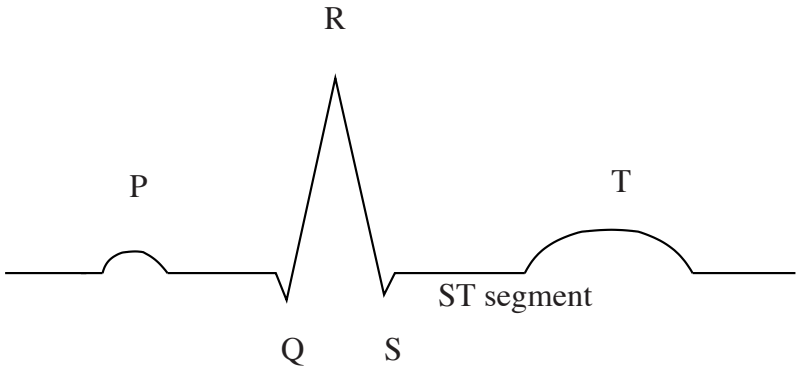

Figure 1.2
Typical waveform of an ECG. The P-wave denotes the atrial depolarization, and the QRS-wave the ventricular depolarization. The T-wave describes the ventricular recovery.

when the membrane becomes permeable, and repolarization is the recovery phase of the ion concentrations returning to normal.

The waveform of the typical ECG is displayed in figure 1.2 with the typical deflections labeled P, QRS, and T, corresponding to atrial contraction (depolarization), ventricular depolarization, and ventricular repolarization, respectively.

The interpretation of an ECG is based on (a) morphology of waves and (b) timing of events and variations observed over many beats.

The diagnostic changes observed in the ECG are permanent or transient occlusion of coronary arteries, heart enlargement, conduction defects, rhythm, and ionic effects.

Electromyogram (EMG)

The electromyogram records the electrical activity of muscles and is used in the clinical environment for the detection of diseases and conditions such as muscular distrophy or disk herniation. There are two types of EMG: intramuscular and surface EMG (sEMG). Intramuscular EMG is performed by inserting a needle which serves as an electrode into the muscle. The action potential represents a waveform of a certain size and shape. Surface EMG (sEMG) is done by placing an electrode on the skin over a muscle in order to detect electrical activity of this muscle.

1.2 Medical Image Analysis

Medical imaging techniques, mostly noninvasive, play an important role in disciplines such as medicine, psychology, and linguistics. The four main medical imaging signals are (1) x-ray transmission, (2) gamma-ray transmission, (3) ultrasound echoes, and (4) nuclear magnetic resonance induction. This is illustrated in table 1.2, where US is ultrasound and MR is magnetic resonance.

Table 1.2
Range of application of the most important radiological imaging modalities [173].

X-rays	Breast, lung, bone
γ-rays	Brain, organ parenchyma, heart function
MR	Soft tissue, disks, brain
US	Fetus, pathological changes, internal organs

The most frequently used medical imaging modalities are illustrated in figure 1.3.

Figure 1.3a and 1.3b illustrate ionizing radiation. Projection radiography and computed tomography are based on x-ray transmission through the body and the selective attenuation of these rays by the body's tissue to produce an image. Since they transmit energy through the body, x-rays belong to transmission imaging modalities, in contrast to emission imaging modalities found in nuclear medicine, where the radioactive sources are localized within the body. They are based on injecting radioactive compounds into the body which finally move to certain regions or body parts, which then emit gamma-rays of intensity proportional to the local concentration of the compounds.

Magnetic resonance imaging is visualized in figure 1.3(c) and is based on the property of nuclear magnetic resonance. This means that protons tends to align themselves with this magnetic field. Regions within the body can be selectively excited such that these protons tip away from the magnetic field direction. The returning of the protons to alignment with the field causes a precession. This produces a radio-frequency (RF) electromagnetic signature which can be detected by an antenna.

Figure 1.3(d) presents the concept of ultrasound imaging: high frequency acoustic waves are sent into the body and the received echoes are used to create an image.

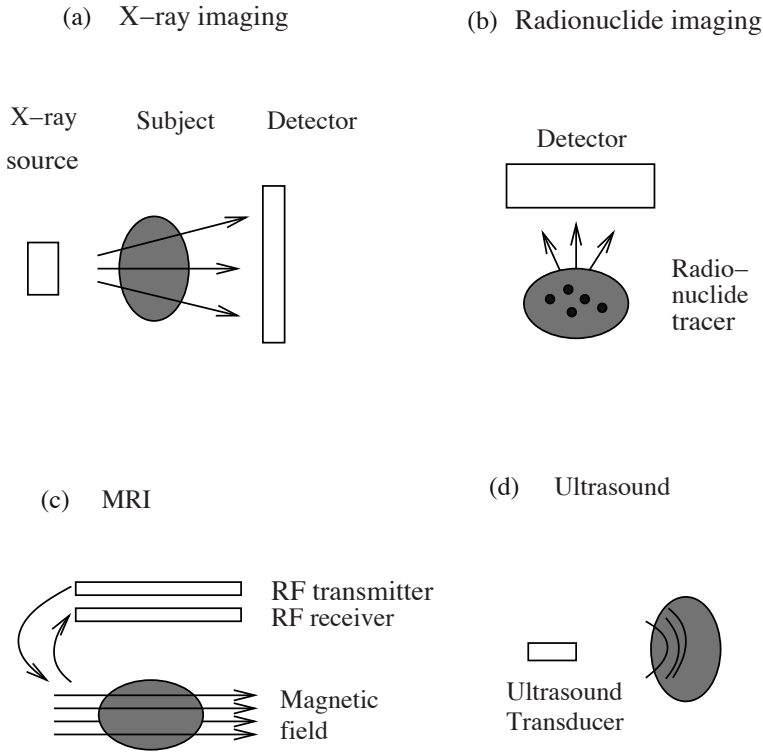

Figure 1.3
Schematic representations of the most frequent used medical imaging modalities [153].

In this chapter, we discuss the four main medical imaging signals introduced in figure 1.3. The medical physics behind these imaging modalities, as well as the image analysis challenges, will be presented. Since the goal of medical imaging is to be automated as much as possible, we will give an overview of computer-aided diagnostic systems in section 1.3. Their main component, the workstation, is described in great detail.

For further details on medical imaging, readers are referred to [51, 164, 280].

Imaging with Ionizing Radiation

X-ray, the most widespread medical imaging modality, was discovered by W. C. Röntgen in 1895. X-rays represent a form of ionizing radiation

with a typical energy range between 25 keV and 500 keV for medical imaging. A conventional radiographic system contains an X-ray tube that generates a short pulse of X-rays that travels through the human body. X-ray photons that are not absorbed or scattered reach the large area detector, creating an image on a film. The attenuation has a spatial pattern. This energy- and material-dependent effect is captured by the basic imaging equation

$$I_d = \int_0^{E_{max}} S_0(E) E \exp\left[- \int_0^d \mu(s; E) ds \right] dE \tag{1.1}$$

where $S_0(E)$ is the X-ray spectrum and $\mu(s; E)$ is the linear attenuation coefficient along the line between the source and the detector; s is the distance from the origin, and d is the source-to-detector distance.

The image quality is influenced by the noise stemming from the random nature of the X-rays or their transmission. Figure 1.4 is a thorax X-ray.

A popular imaging modality is *computed tomography (CT)*, introduced by Hounsfield in 1972, that eliminates the artifacts stemming from overlying tissues and thus hampering a correct diagnosis. In CT, x-ray projections are collected around the patient. CT can be seen as a series of conventional X-rays taken as the patient is rotated slightly around an axis. The films show 2-D projections at different angles of a 3-D body. A horizontal line in a film visualizes a 1-D projection of a 2-D axial cross section of the body. The collection of horizontal lines stemming from films at the same height presents a one-axial cross section. The 2-D cross-sectional slices of the subject are reconstructed from the projection data based on the Radon transform [51], an integral transform introduced by J. Radon in 1917. This transformation collects 1-D projections of a 2-D object over many angles, and the reconstruction is based on a filtered backpropagation, which is the most frequently employed reconstruction algorithm. The projection-slice theorem, which forms the basis of the reconstructions, states that a 1-D Fourier transform of a projection is a slice of the 2-D Fourier transform of the object. Figure 1.5 visualizes this.

The basic imaging equation is similar to conventional radiography, the sole difference being that an ensemble of projections is employed in the reconstruction of the cross-sectional images:

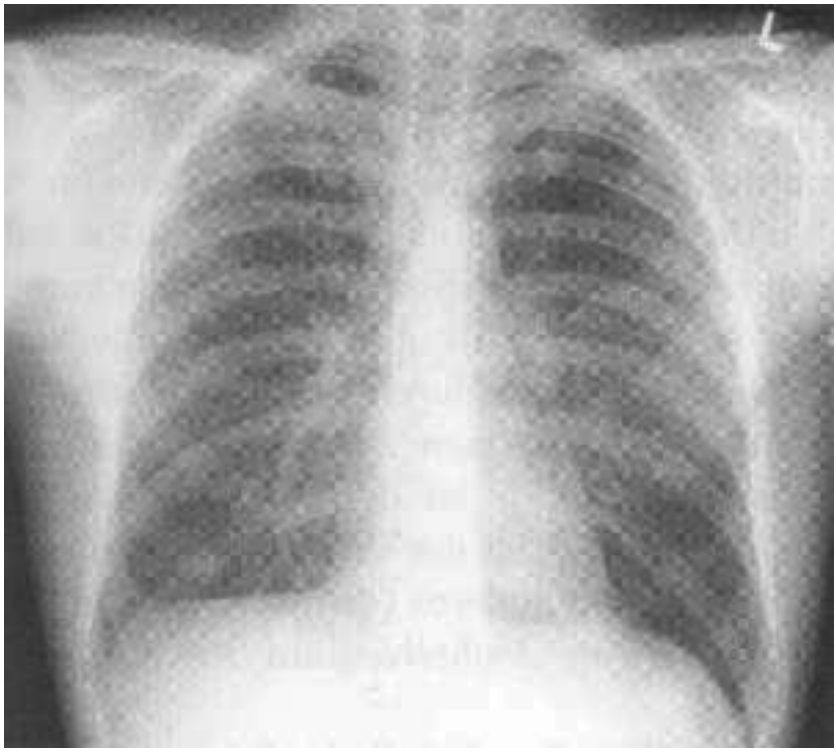

Figure 1.4
Thorax X-ray. (Courtesy of Publicis-MCD-Verlag.)

$$I_d = I_0 \exp\left[-\int_0^d \mu(s;\bar{E})ds\right]dE \tag{1.2}$$

where I_0 is the reference intensity and $\bar{E}$ is the effective energy.

The major advantages of CT over projection radiography are (1) eliminating the superposition of images of structures outside the region of interest; (2) providing a high-contrast resolution such that differences between tissues of physical density of less than 1% become visible; and (3) being a tomographic and potentially 3-D method allowing the analysis of isolated cross-sectional visual slices of the body. The most common artifacts in CT images are aliasing and beam hardening. CT represents an important tool in medical imaging, being used to provide

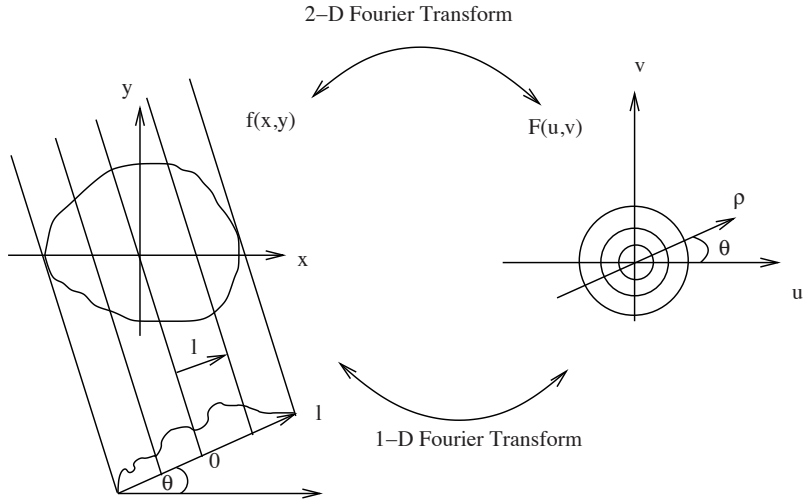

Figure 1.5
Visualization of the projection-slice theorem.

more information than X-rays or ultrasound. It is employed mostly in the diagnosis of cerebrovascular diseases, acute and chronic changes of the lung parenchyma, supporting ECG, and a detailed diagnosis of abdominal and pelvic organs. A CT image is shown in figure 1.6.

Nuclear medicine began in the late 1930s, and many of its procedures use radiopharmaceuticals. Its beginning marked the use of radioactive iodine to treat thyroid disease. Like x-ray imaging, nuclear medicine imaging developed from projection imaging to tomographic imaging. Nuclear medicine is based on ionizing radiation, and image generation is similar to an x-ray's, but with an emphasis on the physiological function rather than anatomy. However, in *nuclear medicine*, radiotracers, and thus the source of emission, are introduced into the body. This technique is a functional imaging modality: the physiology and biochemistry of the body determine the spatial distribution of measurable radiation of the radiotracer. In nuclear medicine, different radiotracers visualize different functions and thus provide different information. In other words, a variety of physiological and biochemical functions can be visualized by different radiotracers. The emissions from a patient are recorded by

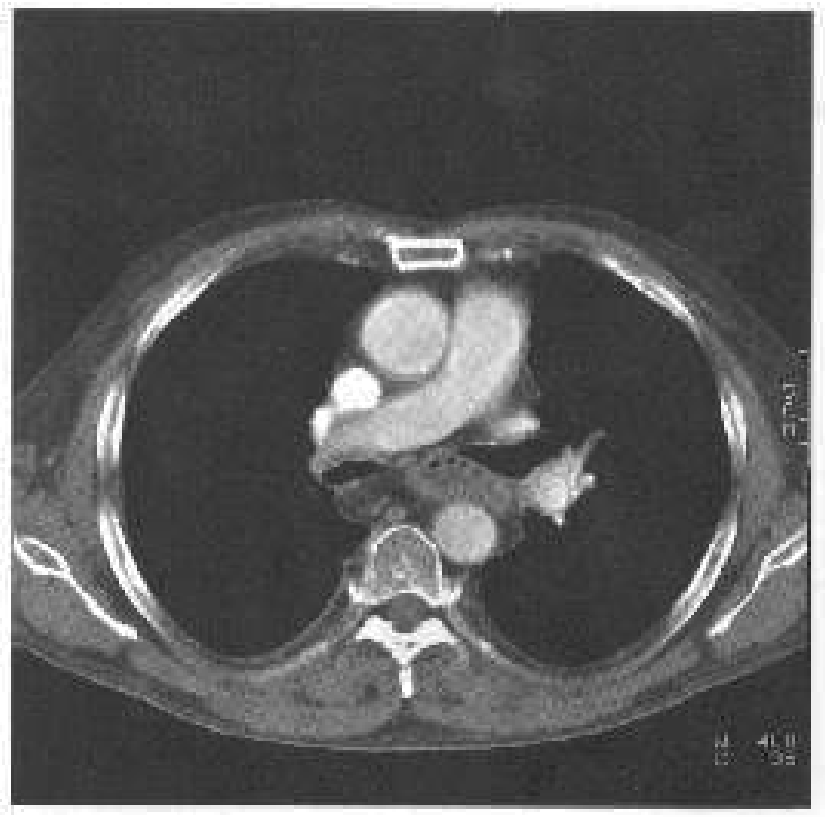

Figure 1.6
CT of mediastinum and lungs. (Courtesy of Publicis-MCD-Verlag.)

scintillation cameras (external imaging devices) and converted into a planar (2-D) image, or cross-sectional images.

Nuclear medicine is relevant for clinical diagnosis and treatment covering a broad range of applications: tumor diagnosis and therapy, acute care, cardiology, neurology, and renal and gastrointestinal disorders.

Based on radiopharmaceutical disintegration, the three basic imaging modalities in nuclear medicine are usually divided into two main areas: (1) planar imaging and *single-photon emission computed tomography (SPECT),* using gamma-emitters as radiotracers, and (2) *positron emission tomography (PET)* using positrons as radiotracers. Projection

imaging, called also planar scintigraphy, uses the Anger scintillation camera, an electronic detection instrument. This imaging modality is based on the detection and estimation of the position of individual scintillation events on the face of an Anger camera. The fundamental imaging equation contains two important components: activity as the desired parameter, and attenuation as an undesired but extremely important additional part.

The fundamental imaging equation is:

$$\varphi(x,y) = \int_{\infty}^{0} \frac{A(x,y,z)}{4\pi z^2} \exp\left(-\int_{z}^{0} \mu(x,y,z';E)dz'\right)dz \tag{1.3}$$

where $A(x,y,z)$ represents the activity in the body and E, the energy of the photon. The image quality is determined mainly by camera resolution and noise stemming from the sensitivity of the system, activity of the injected substance, and acquisition time.

On the other hand, SPECT uses a rotating Anger scintillation camera to obtain projection data from multiple angles. Single-photon emission uses nuclei that disintegrate by emitting a single γ-photon, which is measured with a gamma-camera system. SPECT is a slice-oriented technique, in the sense that the obtained data are tomographically reconstructed to produce a 3-D data set or thin (2-D) slices. This imaging modality can be viewed as a collection of projection images where each is a conventional planar scintigram. The basic imaging equation contains two inseparable terms, activity and attenuation. Before giving the imaging equation, we need some geometric considerations: if x and y are rectlinear coordinates in the plane, the line equation in the plane is given as

$$L(l,\theta) = \{(x,y)|x\cos\theta + y\sin\theta = l\} \tag{1.4}$$

with l being the lateral position of the line and θ the angle of a unit normal to the line. Figure 1.7 visualizes this.

This yields the following parameterization for the coordinates $x(s)$ and $y(s)$:

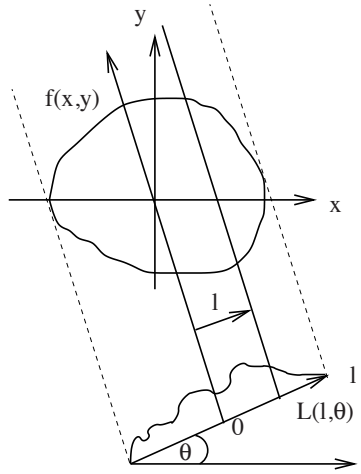

Figure 1.7
Geometric representations of lines and projections.

$$x(s) = l\cos\theta - s\sin\theta \tag{1.5}$$

$$y(s) = l\sin\theta + s\cos\theta \tag{1.6}$$

Thus, the line integral of a function $f(x, y)$ is given as

$$g(l,\theta) = \int_{-\infty}^{\infty} f(x(s), y(s))ds \tag{1.7}$$

For a fixed angle θ, $g(l, \theta)$ represents a projection, while for all l and θ it is called the *2-D radon transformation* of $f(x, y)$.

The imaging equation for SPECT, ignoring the effect of the attenuation term, is:

$$\varphi(l,\theta) = \int_{-\infty}^{\infty} A(x(s), y(s))ds \tag{1.8}$$

where $A(x(s), y(s))$ describes the radioactivity within the 3-D body and is the inverse 2-D Radon transform of $\varphi(l, \theta)$. Therefore, there is no closed-form solution for attenuation correction in SPECT. SPECT represents an important imaging technique by providing an accurate

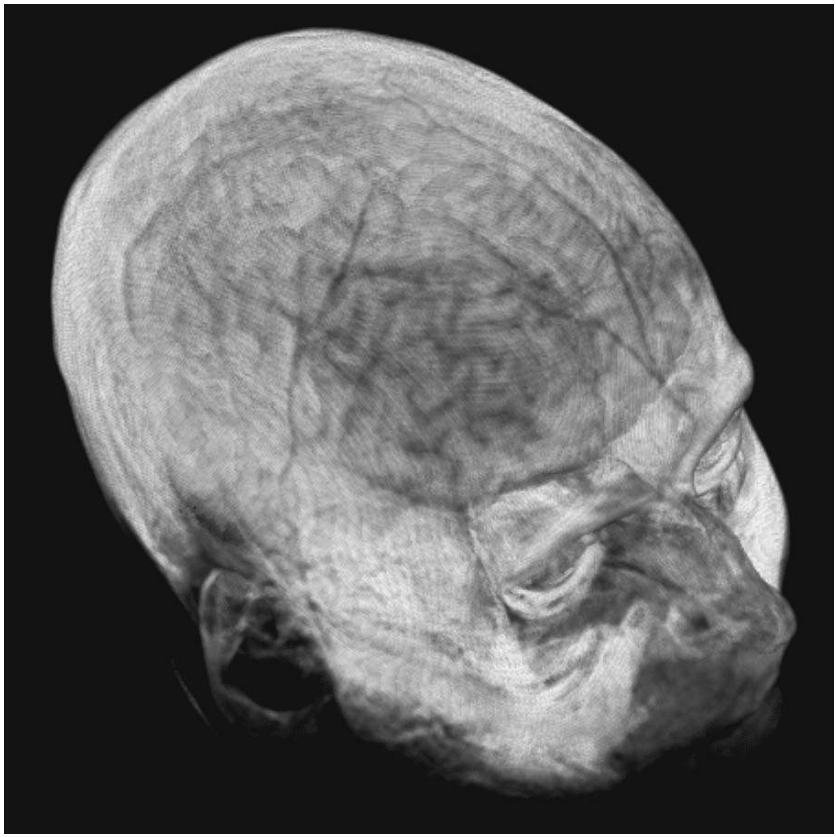

Figure 1.8
SPECT brain study. (Image courtesy Dr. A. Wismüller, Dept. of Radiology, University of Munich.)

localization in 3-D space and is used to provide functional images of organs. Its main applications are in functional cardiac and brain imaging. Figure 1.8 is an image of a SPECT brain study.

PET is a technique having no analogy to other imaging modalities. The radionuclides employed for PET emit positrons instead of γ-rays. These positrons, antiparticles of electrons, are measured and their positions are computed. The reconstruction is produced by using algorithms of filtered backprojection. The imaging equation in PET is similar to that in SPECT, with one difference: The limits of integration for the

attenuation term span the entire body because of the coincidence detection of paired γ-rays, the so-called annihilation photons. The imaging equation is given as

$$\varphi(l,\theta) = K \int_{-R}^{R} A(x(s), y(s))ds \tag{1.9}$$

where K represents a constant that includes the constant factors, such as detector area and efficiency, that influence φ. The image quality in both SPECT and PET is limited by resolution, scatter, and noise. PET has its main clinical application in oncology, neurology, and psychiatry. An important area is neurological disorders, such as early detection of Alzheimers disease, dementia, and epilepsy.

Magnetic Resonance Imaging

Magnetic resonance imaging (MRI) is a non-invasive imaging method used to render images of the inside of the body. Since the late 1970s, it has become one of the key bioimaging modalities in medicine. It reveals pathological and physiological changes in bod tissues as nuclear medicine does, in addition to structural details of organs as CT does.

The MRI signal stems from the nuclear magnetism of hydrogen atoms located in the fat and water of the human body, and is based on the physical principle of nuclear magnetic resonance (NMR). NMR is concerned with the charge and angular momentum possessed by certain nuclei. Nuclei have positive charge and, in the case of an odd atomic number or mass number, an angular momentum Φ. By having spin, these nuclei are NMR-active. Each nucleus that has a spin also has a microscopic magnetic field. When an external electric field is applied, the spins tend to align with that field. This property is called nuclear magnetism. Thus, the spin systems become macroscopically magnetized.

In MR imaging, we look at the macroscopic magnetization by considering a specific spin system (hydrogen atoms) within a sample. The "sample" represents a small volume of tissue (i.e., a voxel). Applying a static magnetic field $\mathbf{B}_0$ causes the spin system to become magnetized, and it can be modeled by a bulk magnetization vector $\mathbf{M}$. In the undisturbed state, $\mathbf{M}$ will reach an equilibrium value $\mathbf{M}_0$ parallel to the direction of $\mathbf{B}_0$, see figure 1.10(a).

It's very important to note that $\mathbf{M}(\mathbf{r}, t)$ is a function of time and

of the 3-D coordinate $\mathbf{r}$ that can be manipulated spatially by external radio-frequency excitations and magnetic fields.

At a given voxel, the value of an MR image is characterized by two important factors: the tissue properties and the scanner imaging protocol. The most relevant tissue properties are the relaxation parameters T_1 and T_2 and the proton density. The proton density is defined as the number of targeted nuclei per unit volume. The scanner software and hardware manipulate the magnetization vector $\mathbf{M}$ over time and space based on the so-called pulse sequence.

In the following text, we will focus on a particular voxel and give the equations of motion for $\mathbf{M}(t)$ as a function of time t. These equations are based on the Bloch equations and describe a precession of the magnetization vector around the external applied magnetic field with a frequency ω_0, which is known as the resonance or Larmor frequency.

The magnetization vector $\mathbf{M}(t)$ has two components:

1. The longitudinal magnetization given by $M_z(t)$, the z-component of $\mathbf{M}(t)$
2. The transverse magnetization vector $M_{xy}(t)$, a complex quantity, which combines two orthogonal components:

$$M_{xy}(t) = M_x(t) + jM_y(t) \tag{1.10}$$

where φ is the angle of the complex number M_{xy}, known as the phase angle, given as

$$\varphi = \tan^{-1} \frac{M_x}{M_y} \tag{1.11}$$

Since $\mathbf{M}(t)$ is a magnetic moment, it will have a torque if an external time-varying magnetic field $\mathbf{B}(t)$ is applied. If this field is static and oriented parallel to the z-direction, then $\mathbf{B}(t) = \mathbf{B}_0$.

The magnetization vector $\mathbf{M}$ precesses if it is initially oriented away from the $\mathbf{B}_0$. The spin system can also be excited by using RF signals, such that RF signals are produced as output by the stimulated system. This RF excitation is achieved by applying $\mathbf{B}_1$ at the Larmor frequency rather than keeping it constant, and allows tracking the position of $\mathbf{M}(t)$. However, the precession is not perpetual, and we will show that there

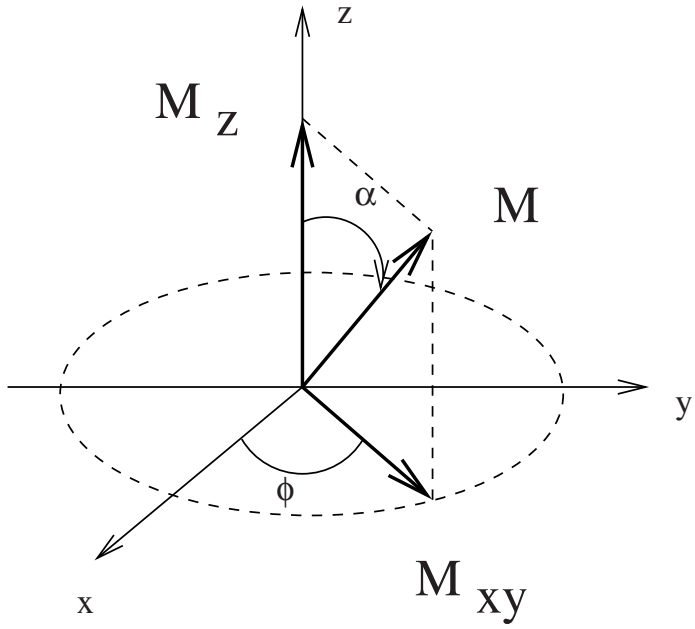

Figure 1.9
The magnetization vector **M** precesses about the z-axis.

are two independent mechanisms to dampen the motion and cause the received signal to vanish: the longitudinal and transversal relaxations.

The RF excitation pushes $\mathbf{M}(t)$ down at an angle α toward the xy-plane if $\mathbf{B}_1$ is along the direction of the y-axis. At $\alpha = 0$, we have $M_z = 0$ and the magnetization vector rotates in the xy-plane with a frequency equal to the Larmor frequency. The $\mathbf{B}_1$ pulse needed for an angle $\alpha = \pi/2$ is called the 90 pulse. The magnetization vector returns to its equilibrium state, and the relaxation process is described by

$$M_z(t) = M_0 \left[1 - \exp\left(-\frac{t}{T_1}\right)\right] \tag{1.12}$$

and depends on the longitudinal or spin-lattice relaxation time (T_1) (See figure 1.9.

Transverse or spin-spin relaxation is the effect of perturbations caused by neighboring spins as they change their phase relative to others. This dephasing leads to a loss of the signal in the receiver antenna. The resulting signal is called free induction decay (FID). The return of the transverse magnetization $\mathbf{M}_{xy}$ to equilibrium is described by

$$M_{xy}(t) = M_{x_0 y_0} \exp\left(-\frac{t}{T_2}\right) \tag{1.13}$$

where T_2 is the spin-spin relaxation time. T_2 is tissue-dependent and produces the contrast in MR images. However, the received signal decays faster than T_2. Local perturbations in the static field $\mathbf{B}_0$ give rise to a faster time constant T_2^*, where $T_2^* < T_2$. Figure 1.10(b) visualizes this situation. The decay associated with the external field effects is modeled by the time constant $T_2^{'}$. The relationship between the three transverse relaxation constants is modelled by

$$\frac{1}{T_2^*} = \frac{1}{T_2} + \frac{1}{T_2^{'}} \tag{1.14}$$

It's important to note that both T_1 and T_2 are tissue-dependent and that for all materials $T_2 \leq T_1$.

Valuable information is obtained from measuring the temporal course of the T1/T2 relaxation process after applying an RF pulse sequence. This measured time course is converted from the time to the frequency domain based on the Fourier transform. The amplitude in the spectrum appears at the resonance frequency of hydrogen nucleons in water (see figure 1.11).

A contrast between tissues can be seen if the measured signal is different in those tissues. In order to achieve this, two possibilities are available: the intrinsic NMR properties, such as P_D, T_1, and T_2, and the characteristics of the externally applied excitation. It is possible to control the tip angle α and to use sophisticated pulse sequences such as the spin-echo sequence. A 90° pulse has a period of TR seconds (repetition time) and is followed by a 180° pulse after TE seconds (echo time). This second pulse partially rephases the spins and produces an echo signal.

Figure 1.12 shows a brain scan as T_1-weighted, T_2-weighted, and hydrogen density-weighted images.

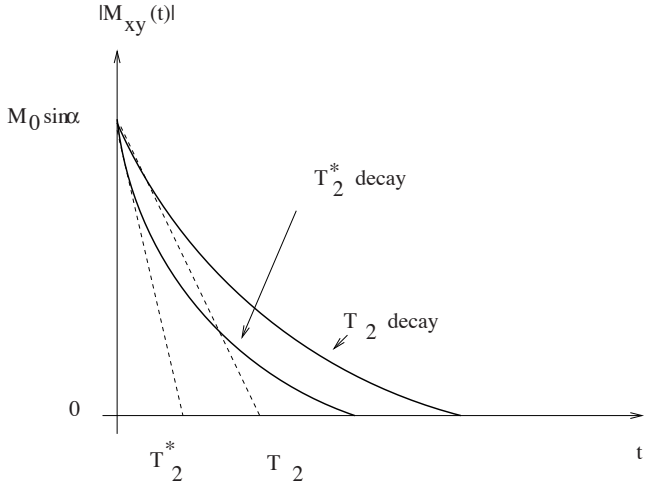

(a)

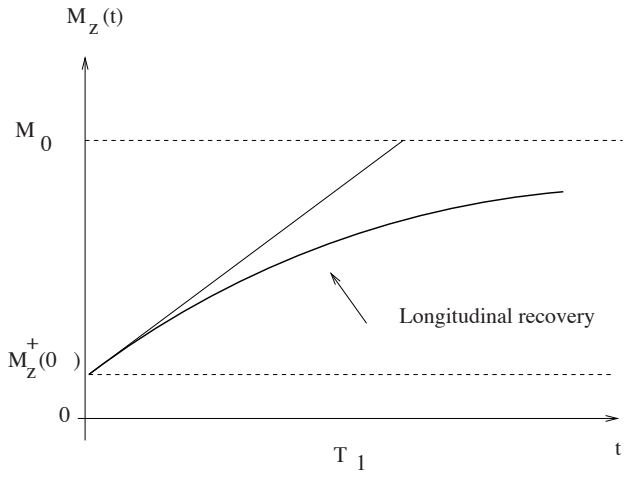

(b)

Figure 1.10
(a) Transverse and (b) longitudinal relaxation.

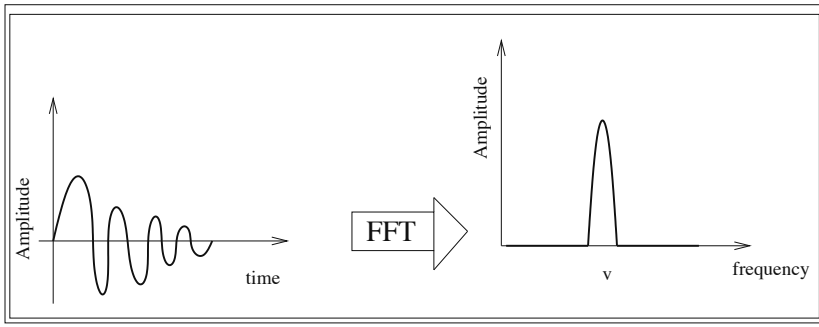

Figure 1.11
Frequency-domain transformation of the measured temporal course. The amplitude in the spectrum is exhibited at the Larmor frequency.

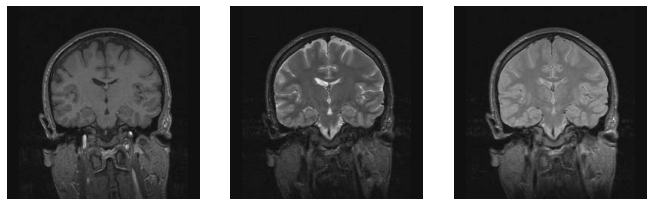

Figure 1.12
Brain MRI showing (a) T_1, (b) T_2, and (c) hydrogen density-weighted images. (Image courtesy Dr. A. Wismüller, Dept. of Radiology, University of Munich.)

"Weighted" means that the differences in intensity observed between different tissues are mainly caused by the differences in T_1, T_2, and P_D, respectively, of the tissues. The basic way to create contrast based on the above parameters is show in table 1.3.

The pixel intensity $I(x, y)$ of an MR image obtained using a spin-echo sequence is given by

$$I(x,y) \propto P_D(x,y) \underbrace{\left(1 - \exp\left[-\frac{T_R}{T_1}\right]\right)}_{\text{T1}-\text{weighting}} \underbrace{\exp\left[-\frac{T_E}{T_2}\right]}_{\text{T2}-\text{weighting}} \tag{1.15}$$

Varying the values of T_R and T_E will control the sensitivity of the signal to the T_1/T_2 relaxation process and will produce different weighted

Table 1.3
Basic way to create contrast depending on P_D, T_1, and T_2.

Contrast	Scanner Parameters
P_D	Long T_R, read FID or use short T_E
T_2	Long T_R, $T_E \approx T_2$
T_1	Read FID or use short T_E, $T_R \approx T_1$

contrast images. If, for example, T_R is much larger than T_1 for all tissues in the *region of interest* (ROI), then the T_1 weighting term converges to zero and there is no sensitivity of the signal to the T_1 relaxation process. The same holds whan T_E is much smaller than T_2 for all tissues. When both T_1 and T_2 sensitivities decrease, the pixel density depends only on the proton density $P_D(x, y)$.

The MR image quality depends not only on contrast but also on sampling and noise. To summarize, the advantages of MRI as an imaging tool are (1) excellent contrasts between the various organs and tumors essential for image quality, (2) the 3-D nature of the image, and (3) the contrast provided by the T_1 and T_2 relaxation mechanism, as one of the most important imaging modalities.

An important technique in MRI is *multispectral magnetic resonance imaging*. A sequence of 3-D MRI images of the same ROI is recorded assuming that the images are correctly registered. This imaging type enables the discrimination of different tissue types.

To further enhance the contrast between tissue types, contrast agents (CA) are used to manipulate the relaxation times. CAs are intravenously administrated, and during that time a signal enhancement is achieved for tissue with increased vascularity.

Functional magnetic resonance imaging (fMRI) is a novel noninvasive technique for the study of cognitive functions of the brain [189]. The basis of this technique is the fact that the MRI signal is susceptible to changes of hemodynamic parameters, such as bood flow, blood volume, and oxygenation, that arise during neural activity. The most commonly used fMRI signal is the blood oxygenation level-dependent (BOLD) contrast. The BOLD temporal response changes when the local deoxyhemoglobin concentration decreases in an area of neuronal activity. This fact is reflected in T_2^*- and T_2-weighted MR images.

The two underlying characteristics of hemodynamic effects are spatial and temporal. While vasculature is mainly responsible for spatial

effects, the temporal effects are responsible for the delay of the detected MR signal changes in response to neural activity and a longer duration of the dispersion of the hemodynamic changes. The temporal aspects impose two different types of fMRI experiments: "block" designs and "event-related" designs. The block designs are characterized by an experimental task performed in an alternating sequence of 20-60 sec blocks. In event-related designs, multiple stimuli are presented randomly and the corresponding hemodynamic response to each is measured. The main concept behind this type of experiment is the almost linear response to multiple stimulus presentations. fMRI, with high temporal and spatial resolution, is a powerful technique for visualizing rapid and fine activation patterns of the human brain. The functional localization is based on the evident correlation between neuronal activities and MR signal changes. As is known from both theoretical estimations and experimental results [187], an activated signal variation appears very low on a clinical scanner. This motivates the application of analysis methods to determine the response waveforms and associated activated regions.

The main advantages of this technique are (1) noninvasive recording of brain signals without any risk of radiation, unlike CT; (2) excellent spatial and temporal resolution, and (3) integration of fMRI with other techniques, such as MEG and EEG, to study the human brain.

fMRI's main feature is to image brain activity in vivo. Therefore its applications lie in the diagnosis, interpretation, and treatment evaluation of clinical disorders of cognitive brain functions. The most important clinical application lies in preoperative planning and risk assessment in intractable focal epilepsy. In pharmacology, fMRI is a valuable tool in determining how the brain is responding to a drug. Furthermore in clinical applications, the importance of fMRI in understanding neurological and psychiatric disorders and refining the diagnosis is growing.

Ultrasound and Acoustic Imaging

Ultrasound is a leading imaging modality and has been extensively studied since the early 1950s. It is a noninvasive imaging modality which produces oscillations of 1 to 10 MHz when passing through soft tissues and fluid.

The cost effectiveness and the portability of ultrasound have made this technique extremely popular. Its importance in diagnostic radiology is unquestionable, enabling the imaging of pathological changes of inner

organs and blood vessels, and supporting breast cancer detection.

The principle of the ultrasonic imaging is very simple: the acoustic wave launched by a transducer into the body interacts with tissue and blood, and some of the energy that is not absorbed returns to the transducer and is detected by it. As a result, "ultrasonic signatures" emerge from the interaction of ultrasound energy with different tissue types that are subsequently used for diagnosis.

The speed of sound in tissue is a function of tissue type, temperature, and pressure. Table 1.4 gives examples of acoustic properties of some materials and biological tissues. Because of scattering, absorption or reflection, an attenuation of the acoustic wave is observed. The attenuation is described by an exponential function of the distance, described by $A(x) = A_0 \exp(-\alpha x)$, where A is the amplitude, A_0 is a constant, α is the attenuation factor, and x is the distance. The important characteristics of the returning signal, such as amplitude and phase, provide pertinent information about the interaction and the type of medium that is crossed. The basic imaging equation is the pulse-echo equation, which gives a relation among the excitation pulse, the transducer face, the object reflectivity, and the received signal.

Ultrasound has the following imaging modes:

- A-mode (amplitude mode): the most simple method that displays the envelope of pulse-echoes versus time. It is mostly used in ophthalmology to determine the relative distances between different regions of the eye, and also in localization of the brain midline or of a myocardial infarction. Figure 1.13 visualizes this aspect.
- B-mode (brightness mode): produced by scanning the transducer beam in a plane, as shown in figure 1.14. It can be used for both stationary and moving structures, such as cardiac valve motion.
- M-mode (motion mode): displays the A-mode signal corresponding to repeated pulses in a separate column of a 2-D image. It is mostly employed in conjunction with ECG for motion of the heart valves.

The two basic techniques used to achieve a better sensitivity of the echoes along the dominant (steered) direction are the following:

- Beam forming: increases the transducer's directional sensitivity
- Dynamic focusing: increases the transducer's sensitivity to a particular point in space at a particular time

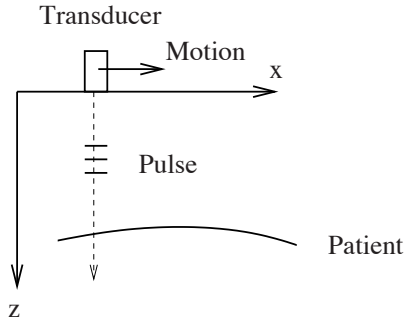

Figure 1.13
A-mode display.

Table 1.4
Acoustical properties of some materials and biological tissues .

Medium	Speed of sound (m/sec)	Impedance (10^6kg/m^2s)	Attenuation (dB/cm at 1MHZ)
Air	344	0.0004	12
Water	1480	1.48	0.0025
Fat	1410	1.38	0.63
Muscle	1566	1.70	1.2-3.3
Liver	1540	1.65	0.94
Bone	4080	7.80	20.0

1.3 Computer-Aided Diagnosis (CAD) Systems

The important advances in computer vision, paired with artificial intelligence techniques and data mining, have facilitated the development of automatic medical image analysis and interpretation. Computer-aided diagnosis (CAD) systems are the result of these research endeavors and provide a parallel second opinion in order to assist clinicians in detecting abnormalities, predicting the diseases progress, and obtaining a differential diagnosis of lesions.

Modern CAD systems are becoming very sophisticated tools with a user-friendly graphical interface supporting the interactions with clinicians during the diagnostic process. They have a multilayer architecture with many modules, such as image processing, databases, and a graphical interface.

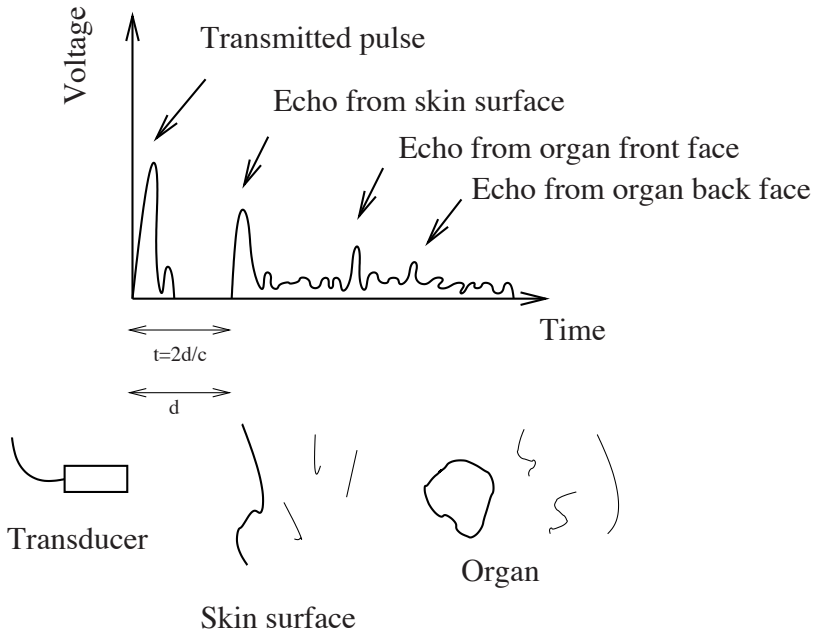

Figure 1.14
B-mode scanner.

A typical CAD system is described in [205]. It has three layers: data layer, application layer, and presentation layer, as shown in figure 1.15.

The functions of each layer are described below.

• Data layer: has a database management system which is responsible for archiving and distributing data

• Application layer: has a management application server for database access and presentation to graphical user interface, a WWW server to ensure remote access to the CAD system, and a CAD workstation for image processing

• Presentation layer: has the Eeb viewer to allow a fast remote access to the system, and at the user site it grants access to the whole system.

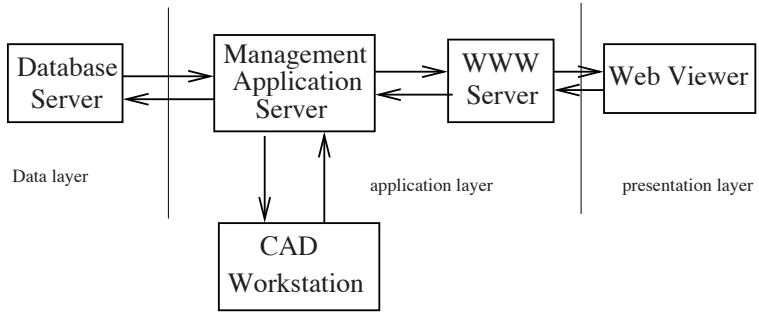

Figure 1.15
Multilayer structure of a CAD system [205].)

CAD Workstation

A typical CAD system's architecture is shown in figure 1.16. It has four important components: (1) image preprocessing, (2) definition of a region of interest (ROI), (3) extraction and selection of features, and (4) classification of the selected ROI.

These basic components are described in the following:

• Image preprocessing: The goal is to improve the quality of the image based on denoising and enhancing the edges of the image or its contrast. This task is crucial for subsequent tasks.

• Definition of an ROI: ROIs are mostly determined by growing seeded regions and by active contour models that correctly approximate the shapes of organ boundaries.

• Extraction and selection of features: These are crucial for the subsequent classification and are based on finding mathematical methods for reducing the sizes of measurements of medical images. Feature extraction is typically carried out in the spectral or spatial domains and considers the whole image content and maps it onto a lower-dimensional feature space. On the other hand, feature selection considers only the information necessary to achieve a robust and accurate classification. The methods employed for removing redundant information are exhaustive, heuristic, or nondeterministic.

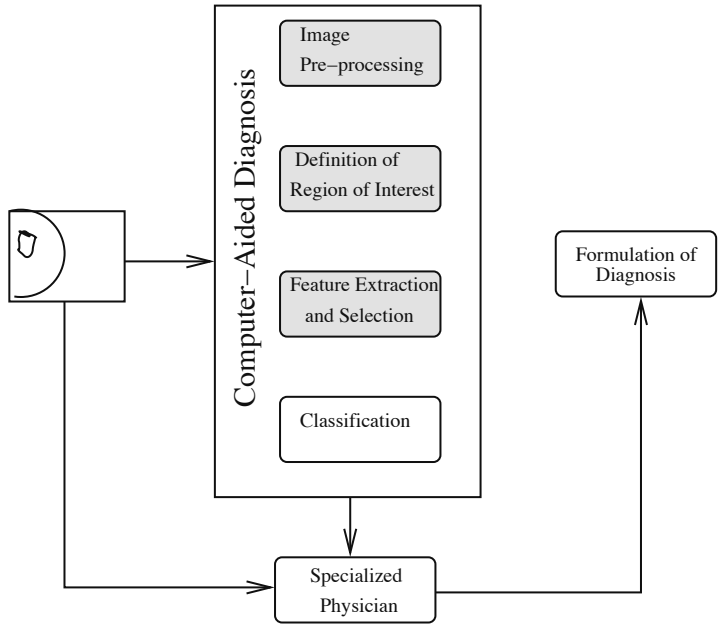

Figure 1.16
Typical architecture of a CAD workstation.

• Classification of the selected ROI: Classification, either supervised or unsupervised, assigns a given set of features describing the ROI to its proper class. These classes can be in medical imaging of tumors, diseases, or physiological signal groups. Several supervised and unsupervised classification algorithms have been applied in the context of breast tumor diagnosis [171, 201, 294].